

## NEAR WAKE CHARACTERISTICS OF CIRCULAR CYLINDERS ARRANGED IN A NON-CONNECTING CRUCIFORM GEOMETRY

T.A. FOX

Department of Civil Engineering,  
University of Queensland, St. Lucia, Qld. 4067  
AUSTRALIA

### ABSTRACT

The complex turbulent flow regimes established in the near wake of circular cylinders arranged in a non-connecting cruciform geometry have been investigated by undertaking a wind tunnel study. The configuration was immersed in a steady, low-turbulence, uniform airflow and studied at a Reynolds number of  $2 \times 10^4$  (based on cylinder diameter and freestream velocity). It was found that two fundamental regimes are possible at the centre of the geometry and that these are dependent upon the spacing of the cylinders. When the distance between the axis of each cylinder is less than three diameters, fluid motion in the central near wake is dominated by secondary flows associated with trailing vortices and horseshoe vortices, whereas at spacings beyond this critical value there is a considerable reduction in the influence of secondary flow.

### INTRODUCTION

Fluid flows associated with bluff bodies often exhibit complex turbulent regimes which are of practical significance. Such a fluid motion is created when a uniform flow is forced to pass around a configuration composed of circular cylinders arranged perpendicular to each other in a cruciform geometry. Indeed, in the wake of this type of obstruction a turbulent three-dimensional flow field is created which has importance in a wide range of engineering applications. For example, this type of configuration is often found in lattice frameworks exposed to a wind or marine environment, or in grids used for the control of turbulence levels in wind tunnel studies, and may be utilized in thermal cooling devices.

Despite the widespread use of cruciform geometries composed of circular cylinders, the associated flow regimes have only received attention in a small number of recent studies. Osaka et al (1983a, b) and Zdravkovich (1985) have examined the fluid motion induced by two cylinders which intersect in a single plane to form a cross, and Zdravkovich (1983) and Tomita et al (1987) have determined details of the flow around two cylinders placed one behind the other to form a cruciform geometry with a point of contact. In each case these authors found that the overall flow field can be divided into two characteristic regions. These are, an outer region of quasi two-dimensional flow, and an inner region of highly three-dimensional conditions in close proximity to the centre of the geometry.

This paper considers the effect upon these regions of the introduction of a gap at the centre of the geometry for the case of non-connecting cylinders with axis spacings up to ten diameters.

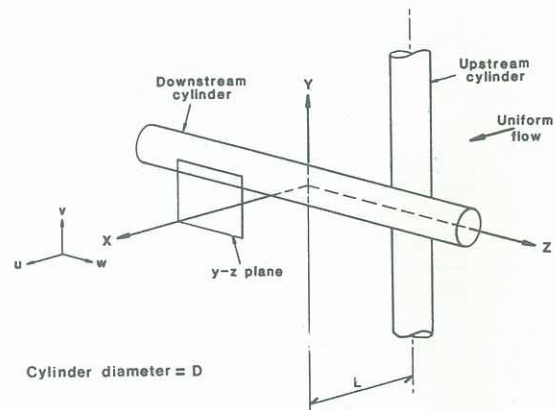


Figure 1: Cruciform geometry and co-ordinates.

### EXPERIMENTAL DETAILS

The experimental measurements were made in a low-speed, blow down, open circuit wind tunnel facility in the Department of Civil Engineering at the University of Surrey in the United Kingdom. This has working section dimensions of 1.067m width x 1.372m height x 9.0m length and produces a uniform airflow with a freestream turbulence intensity of 0.17% at the model testing station.

Two smooth surface aluminium circular cylinders of 30mm diameter formed the cruciform geometry which completely spanned the working section in the vertical and horizontal directions. The vertical cylinder could be displaced to establish a gap at the centre of the configuration as illustrated in Figure 1. The latter also shows the co-ordinate system based on this geometry and defines the separation distance,  $L$ . The blockage associated with each member was 2.2% and 2.8% for the horizontal and vertical cylinders respectively. These values were considered sufficiently low for it to be unnecessary to apply a correction factor to the experimental data.

Mean surface pressure distributions were measured by the use of 0.5mm diameter tappings connected to a low-pressure transducer via a Scanivalve switch mechanism. The latter was controlled by a microcomputer, which also performed data acquisition and on-line analysis. The freestream reference pressure was obtained from a pitot-static tube positioned in the uniform flow. Values of the coefficient of pressure,  $C_p$ , were calculated with an accuracy of 1.5% by the use of

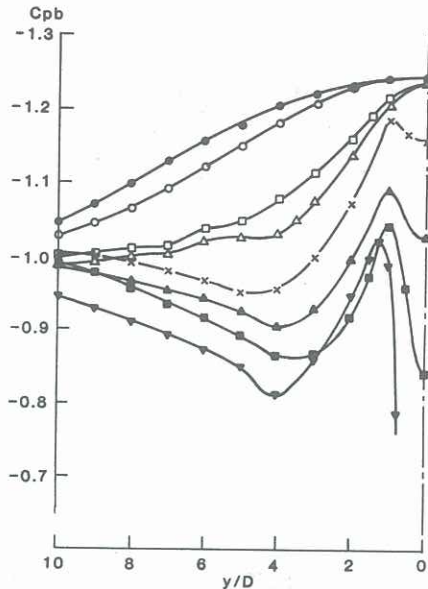


Figure 2: Mean base pressure distributions on the upstream cylinder;  $\nabla$  1.5,  $\blacksquare$  2.0,  $\blacktriangle$  2.5,  $\times$  3.0,  $\Delta$  4.0,  $\square$  5.0,  $\circ$  10.0,  $\bullet$  single cylinder.

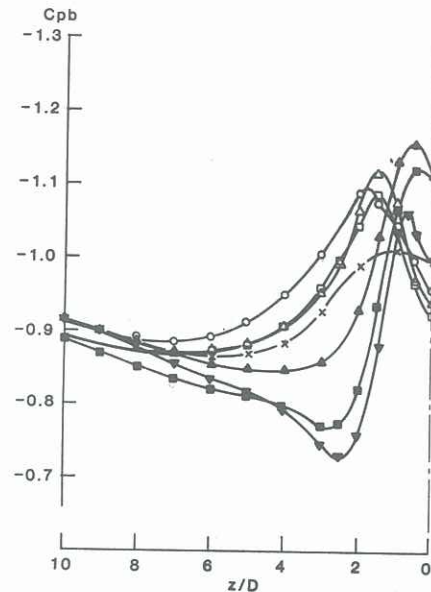


Figure 3: Mean base pressure distributions on the downstream cylinder;  $\nabla$  1.5,  $\blacksquare$  2.0,  $\blacktriangle$  2.5,  $\times$  3.0,  $\Delta$  4.0,  $\square$  5.0,  $\circ$  10.0.

this method in accordance with the expression:

$$C_p = \frac{P_L - P_0}{0.5 \rho U_0^2}$$

where  $P_L$  is the local surface pressure,  $P_0$  is the freestream static pressure, and  $0.5 \rho U_0^2$  is the dynamic head of the freestream.

Velocity and turbulence intensity data was obtained with a pulsed-wire anemometer of the type described by Bradbury and Castro (1971), this being an appropriate instrument for use in highly turbulent flows. Data collection over the near wake was achieved by mounting the probe on a three-dimensional traversing system, which has a positional accuracy of  $\pm 0.02$ mm. On-line data acquisition and analysis was performed by the microcomputer, values of the velocity components and turbulence intensities being calculated from the mean of 10,000 samples taken at each measurement position.

In order to calculate the distribution of X-direction vorticity,  $\omega_x$ , over related planes in the wake, it was necessary to obtain normalized mean velocity components;  $\bar{u}/U_0$ ,  $\bar{v}/U_0$  and  $\bar{w}/U_0$ . To achieve this, each two-dimensional traverse over the measurements plane was repeated five times with the probe at yaw angles of  $0^\circ$  and  $\pm 45^\circ$ , and the data was reduced by the method of Cheun (1981). From these results an approximate differentiation of the mean velocity profiles was undertaken to give the X-direction vorticity:

$$\omega_x = \frac{\partial \bar{w}}{\partial y} - \frac{\partial \bar{v}}{\partial z}$$

## RESULTS AND DISCUSSION

The experiments were undertaken at a Reynolds number of  $Re = 2 \times 10^4$  based on the cylinder diameter and freestream velocity. This value, which is in the upper subcritical range associated with a circular cylinder, was chosen for its practical significance and compatibility with previous work performed in this field.

Mean pressure distributions measured on the base centre-line of the upstream cylinder over half of the span (symmetry about the centre-line is assumed), for a range of spacings from  $L=1.5D$  to  $L=10D$ , are presented in Figure 2. These can be divided into two groups which are dependent upon the distance separating the cylinders. In the first group, when the spacing is in the range  $L \leq 3D$ , the distributions exhibit an outer region of relatively undisturbed conditions and an inner region of interference effects in close proximity to the centre of the geometry. The latter region is characterized by a local peak in suction at  $y/D \approx 1.0$ , with associated pressure gradients which are a result of strong secondary flows at the rear surface of the cylinder. Such flows were identified in visualization experiments performed by Zdravkovich (1983) which revealed the existence of two intense trailing vortices, one either side of the base centre-line, at a similar location on a cruciform geometry composed of two cylinders in contact ( $L=1D$ ). Figure 2 suggests that similar trailing vortices are generated at cylinder spacings up to  $L=3D$ , and that they are sustained by ventilation of fluid towards the point of peak suction.

As the separation distance between the two cylinders increases towards the critical value, the pressure gradients on the base centre-line show a considerable reduction in secondary flow in the disturbed inner region until eventually, at  $L > 3D$ , the peak suction adjacent to the centre of the span is no longer evident. With increased spacing in this second range the pressure profiles tend towards that recorded on a single cylinder.

Strong secondary flows in a highly disturbed inner region are also evident in the spanwise distributions of base pressure recorded on the surface of the downstream cylinder, Figure 3. At cylinder spacings in the range  $L < 3D$  the distributions exhibit a peak in suction adjacent to the centre of the geometry which initially appears to be similar to that recorded on the upstream cylinder at corresponding spacings. However, closer inspection reveals two significant differences. These are that the position of peak

suction is closer to the centre of the span, at  $z/D=0.5$ , and that the region of highly disturbed conditions is reduced in spanwise extent. Zdravkovich (1983) also found the inner region of gross interference to the flow conditions around the downstream member of the cylinders in contact configuration to be restricted to a shorter proportion of the span. In the latter case, visualization of the surface flow patterns revealed this apparent reduction in the extent of the interference effects to be due to the generation of two horseshoe vortices, one from each side of the point of contact, which remain attached to the surface of the downstream cylinder as they converge in the wake. The results presented in Figure 3 show that this regime persists for spacings over the range  $L < 3D$ .

When the distance between the axis of each cylinder is three diameters the distributions in Figure 3 alter significantly. In this respect the suction peak recorded on the base centre-line shifts to a position further from the centre of the geometry, and the profile shape resembles that associated with the upstream cylinder at spacings in the range  $L \leq 3D$ . This regime persists for further increases in cylinder spacing over the range examined (up to ten diameters).

The main features of the spacing related flow regimes discussed above were examined in flow visualization studies and are summarized in Figure 4. When the distance between the axis of each cylinder is less than three diameters, Figure 4(a), four trailing vortices are generated, one in each quadrant of the geometry, and a pair of horseshoe vortices develop around the centre-line of the downstream cylinder. At spacings of  $L > 3D$ , the horseshoe vortices are replaced by weaker circulations, as shown in Figure 4(b), and the trailing vortices cease to exist, the conditions being quasi two-dimensional along the whole upstream span.

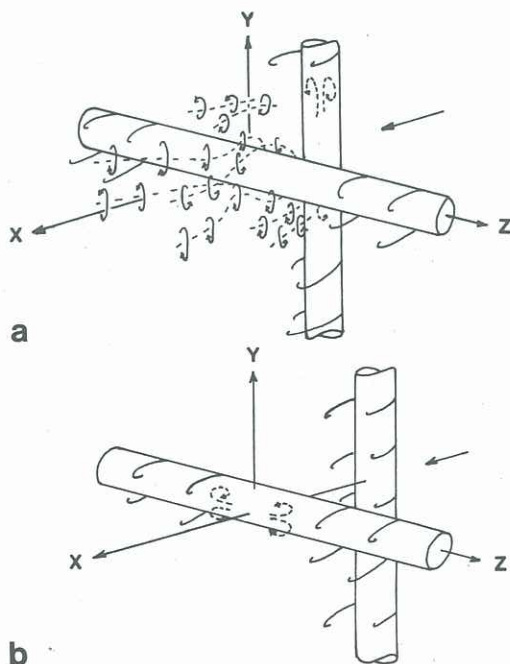


Figure 4: Spacing related flow regimes in the near wake; (a)  $L < 3D$ , (b)  $L > 3D$ .

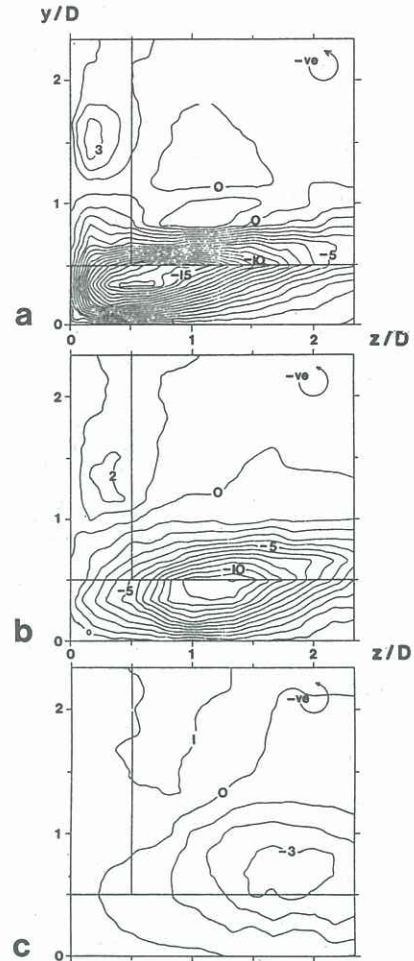


Figure 5: Distribution of X-direction vorticity in the near wake when  $L=2D$ ; (a)  $x=1D$ , (b)  $x=2D$ , (c)  $x=4D$ . (Contours =  $10D\omega_x/U_0$ ).

To examine in detail the complex secondary flow regime that occurs in the near wake of the cruciform configuration at spacings in the range  $L < 3D$ , distributions of vorticity were determined in  $y-z$  planes covering one quadrant of the geometry (see Figure 1). These planes were located at  $x=1D$ ,  $x=2D$ , and  $x=4D$  downstream of the configuration with a cylinder spacing of  $L=2D$ . The results are presented in Figure 5 and show that at  $x=1D$  two dominant areas of secondary flow are present which correspond to the near wake regimes illustrated in Figure 4(a). In this respect the intense circulation with its centre at  $z/D=0.5$ ,  $y/D=0.25$  is associated with one of the horseshoe vortices, and the weaker circulation centred on  $z/D=0.25$ ,  $y/D=1.5$  corresponds to a trailing vortex.

In the case of the horseshoe vortex, the location of the centre of secondary flow in the  $y-z$  plane at  $x=1D$  coincides with the position of the suction peak recorded at  $z/D=0.5$  on the base centre-line of the downstream cylinder, Figure 3, and the direction of the circulation is compatible with the associated pressure gradients. However, Figure 5(b) and (c) show that this centre of maximum vorticity moves laterally away from the centre of the configuration in the near wake, it being located at  $z/D=1.75$ ,  $y/D=0.7$  by  $x=4D$ . In addition the vortex is seen to decay rapidly during this migration, the maximum vorticity recorded at  $x=4D$  being only 20% of that found in the immediate wake at  $x=1D$ .

The effect of these secondary flow regimes upon the distribution of longitudinal turbulent intensity,  $u^2/U_0^2$ , at  $x=1D$ ,  $x=2D$  and  $x=4D$  in the near wake can be assessed through Figure 6. At each downstream location the general contour pattern in the quadrant is influenced to a large degree by the perpendicular arrangement of the members and, in respect of this, the result is similar to that found by Osaka et al (1983,b) in the wake of intersecting cylinders forming a cross. Indeed, the latter investigation revealed a cross pattern in the turbulence intensities measured in the wake at  $x=30.5D$ , with a maximum intensity at the centre of the distribution.

In the case of non-connecting cylinders, Figure 6 shows the peak intensity recorded in the immediate wake ( $x=1D$ ) to be similarly located close to the centre of the configuration and, as such, coincident with the position of the horseshoe vortex. However, the contours in the region  $z/D > 1$  are parallel to the axis of the downstream cylinder at  $x=1D$  and  $x=2D$  and are indicative of the position of the free shear layer separated from that member. This suggests that a quasi two-dimensional vortex shedding process dominates the wake in this region despite the presence of

secondary flow associated with the horseshoe vortex. Indeed, Zdravkovich (1983) recorded a Strouhal number compatible with a von Kármán street at a similar location in the wake of the downstream member of the cruciform cylinders forming a point of contact geometry.

A dominant quasi two-dimensional structure can also be deduced from the parallel contours in the wake of the upstream cylinder at  $y/D > 1$ . In this case, further evidence for such a regime is provided in the flow visualization work undertaken by Tomita et al (1987), which revealed a von Kármán street in the  $x-z$  plane at  $y/D=2.7$  in the wake of the upstream cylinder when  $L=1.67D$ .

#### CONCLUSIONS

The results of an experimental investigation have provided details of the near wake characteristics of non-connecting cylinders arranged in a cruciform geometry. It was found that complex three-dimensional flow regimes occur at the centre of the configuration, the precise nature of which are dependent upon the spacing of the cylinders. If the distance between the axis of each cylinder is less than three diameters,  $L < 3D$ , four trailing vortices are generated, one in each quadrant of the geometry, and a pair of horseshoe vortices develop around the centre of the downstream cylinder. These secondary flows cause a gross disturbance to the flow conditions close to the centre of the span, whereas at spanwise locations away from the centre the wake is dominated by quasi two-dimensional conditions. When the axis spacing is in excess of three diameters,  $L > 3D$ , there is a considerable reduction in the influence of secondary flows in the wake.

#### ACKNOWLEDGEMENT

The author wishes to acknowledge the supervision of Dr. N. Toy in connection with this work which was supported through an S.E.R.C. Studentship.

#### REFERENCES

- Bradbury, L.J.S. and Castro, I.P. (1971) A pulsed wire technique for velocity measurements in highly turbulent flows. *J. Fluid Mech.*, 49, pp657-691.
- Cheun, B.S. (1981) Separated shear layers behind two-dimensional square-edged bodies. Ph.D. Thesis, University of Surrey.
- Osaka, H., Nakamura, I., Yamada, H., Kuwata, Y. and Kageyama, Y. (1983a) The structure of a turbulent wake behind a cruciform circular cylinder, 1st report: The mean velocity field. *Bull. Jpn. Soc. Mech. Engrs*, 26, pp356-363.
- Osaka, H., Yamada, H., Nakamura, I., Kuwata, Y., and Kageyama, Y. (1983b) The structure of a turbulent wake behind a cruciform circular cylinder, 2nd report: The streamwise development of turbulent flow fields. *Bull. Jpn. Soc. Mech. Engrs*, 26, pp521-528.
- Tomita, Y., Inagaki, S., Suzuki, S. and Muramatsu, H. (1987) Acoustic characteristics of two circular cylinders forming a cross in uniform flow. *J.S.M.E. Int. Journal*, 30, pp1069-1079.
- Zdravkovich, M.M. (1983) Interference between two circular cylinders forming a cross. *J. Fluid Mech.*, 128, pp231-246.
- Zdravkovich, M.M. (1985) Flow around two intersecting circular cylinders. *Trans. ASME: J. Fluid Engng*, 107, pp507-511.

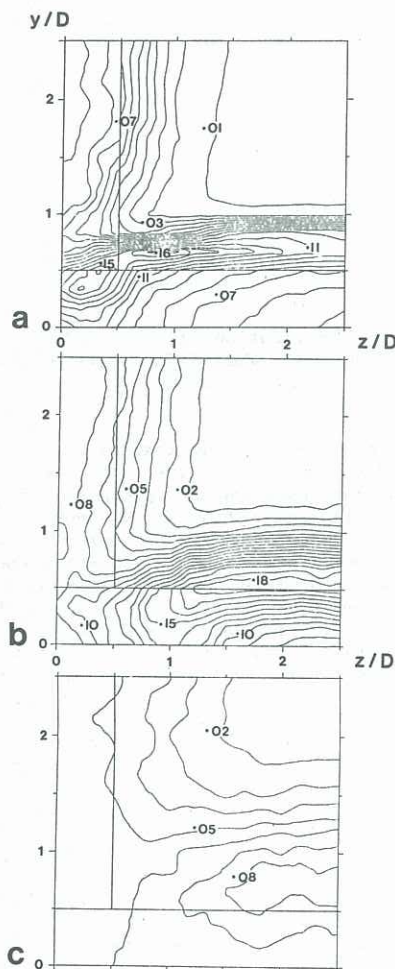


Figure 6: Distribution of turbulence intensity  $u^2/U_0^2$ , in the near wake when  $L=2D$ ; (a)  $x=1D$ , (b)  $x=2D$ , (c)  $x=4D$ .